Electronic Supplementary Material (ESI) for Nanoscale.

Supplementary Information

Bottom-up Meets Top-down: Tailored Raspberry-like Fe_3O_4-Pt Nanocrystal Superlattices

Fen Qiu,[a †] René H. J. Vervuurt,[b †] Marcel A. Verheijen,[b,c] Edmond W. Zaia,[a,d] Erin B. Creel,[a,d]

Youngsang Kim,[a] Jeffrey J. Urban,*[a] Ageeth A. Bol*[b]

Table of contents

1. Experimental Section

1.1. Synthesis of Fe_3O_4: Fe_3O_4 NPs were synthesized under argon atmosphere using standard Schlenk line techniques according to the literature method.[1]

1.2. Self-assembly of Fe_3O_4 superlattices: a solution of Fe_3O_4 NPs was drop-cast onto the surface of diethylene glycol (DEG) in a Teflon well swiftly, and covered with glass to ensure a slow evaporation of solvent form a film. Silicon monoxide TEM grids were used here for transferring the fluid supported film upon drying of the NP solvent for the studies in this report.

1.3. Atomic Layer Deposition: Pt was deposited on the Fe_3O_4 super lattices by ALD, in a home-built ALD reactor equipped with an inductively coupled plasma (ICP) source.[2] The base pressure of the system was ~10^{-6} mbar. Before ALD the Fe_3O_4 particles were cleaned by a 3 min O_2 plasma exposure (0.01 mbar, 100W), to remove any remaining oleylamine and oleic acid ligands form the Fe_3O_4 super lattice synthesis process. Due to carbon build up on the samples as a result of air exposure, it is difficult to confirm the removal of these ligands with any ex-situ technique, for example, XPS. It should be noted that without O_2 pre-treatment no uniform Pt particle growth on the Fe_3O_4 was obtained, which is an indirect proof that some, if not all carbon has been removed. Additionally, without O_2 pre-treatment a low contrast (low-atomic number) shell could sometimes be observed around the particles in TEM, possibly indicating the remnants of the ligand molecules, shown in Figure S7 in SI After plasma treatment this shell was no longer observed and the Pt growth was uniform across the sample.

The Pt ALD process consisted of a 4 s $MeCpPtMe_3$ precursor dose and a 5 s O_2 gas reaction step, separated by pump steps. The table temperature was set to 300 °C, while the reactor walls were kept at 100 °C. The effective sample temperature during deposition was approximately 120 °C, as determined by *in-situ* spectroscopic ellipsometry (SE) using a Si reference sample. The O_2 pressure during the reaction step was 0.01 mbar. The relatively low pressure during Pt deposition results in a poor thermal contact between the substrates used and the table heater. The effective

sample temperature is therefore much lower than 300 °C and closer 120 °C, as determined by *in-situ* spectroscopic ellipsometry (SE) using a Si reference sample. The low sample temperature prevents Pt growth on the SiO_2 substrates, making the selective deposition of Pt on Fe_3O_4 possible.[3] This is because the thermal energy is insufficient to dissociate O_2 and remove the $MeCpPtMe_3$ precursor ligands in the O_2 half cycle on SiO_2.[4] Pt growth does occur on the Fe_3O_4 particles, most likely due to its catalytic properties, such as its ability to dissociate H_2O.[5] For some of the experiments the Pt ALD deposition was interrupted by a 3 min O_2 Plasma exposure (0.01 mbar, 100W) to remove surface carbon that accumulated on the Pt and Fe_3O_4 during growth.

1.4. Transmission electron microscope (TEM): TEM images were acquired on an CM200 operated at 200 keV.

1.5. Scanning transmission electron microscope (STEM): After Pt ALD the samples were analyzed by a JEOL ARM 200 probe corrected STEM, operated at 200 kV. The images were acquired in high angle annular dark field (HAADF) mode. The Pt particle size was determined by analyzing several (minimum of 3 per sample) HAAFD STEM images using the Image J software package.

1.6. X-ray Photoelectron Spectroscopy: X-ray Photoelectron Spectroscopy (XPS) was used to investigate the electronic structure of the Pt-Fe3O4 composite nanoparticle system. Specifically, the Pt 4f and Fe 2p core levels were probed. A PHI 5400 X-ray Photoelectron Spectroscopy (XPS) System with a conventional Mg Kα source operated at 350 W was used for this purpose. Pass energy of 20 eV was used for narrow scan spectra, corresponding to an energy resolution of ~700 meV. All peak positions were referenced to the C 1s of 284.5 eV.

1.7. Fabrication of Electrode: A circular glass substrate (19 mm diameter and 0.5 mm thick, ProSciTech) was cleaned using solvents (acetone and isopropyl alcohol) followed by ultrapure water (Milli-Q) then air plasma (for 3 min). The air plasma cleaning enhances the adhesion of metals on the glass. Ag and Ti was deposited using an e-beam evaporator through a shadow

mask having a dumbbell-like shape, where Ti (3 nm thick) is used to promote the adhesion of Ag thin film (100 nm thick) to the glass. Subsequently, on top of Ag thin film, TiO_2 film (80 nm thick) was deposited using an e-beam evaporator except the contact area. The substrate temperature kept 350˚C while depositing TiO_2.

1.8. Photocurrent measurement: We have built a highly sensitive photocurrent measurement setup for the electrochemical cell system using the lock-in technique. A sample immersed in a glass electrochemical cell with a quartz window is illuminated by a light source (Xe lamp, ~ 850 mW/cm^2) through a condenser lens (transmission: 350 nm – 700 nm) and a chopper. The light chopping (3 Hz) is synchronized with a lock-in amplifier (SRS 850) to lock-in the square wave of modulated photocurrent generated by the chopped light. The lock-in amplifier is also linked with a potentiostat (BioLogic SP-200). The lock-in amplifier generates the r.m.s. amplitude of the first harmonic of the signal, which is the photocurrent. In this manner, we can measure the amplitude of photocurrent while sweeping the potential applied to the working electrode. The condenser lens that blocks IR wavelengths and the light chopping in a short period rule out any heating effect on the surface of our samples.

1.9. IPCE measurements: Incident to photon-to-current efficiency (IPCE) is a potential-dependent measurement of how efficiently photons of a given wavelength are converted to charge transfer in an electrochemical cell (three electrode configuration). A highly-sensitive IPCE setup was built incorporating the lock-in technique with a potentiostat (Biologic SP-200) and a monochromator (Oriel Cornerstone 130). A visible wavelength of light from a Xe lamp is selected by a monochromator and illuminates the photoelectrode surface through a chopper. The on and off pattern of illumination created by the chopper generates a 3 Hz square wave signal which is fed into the lock-in amplifier for enhanced signal-to-noise ratio. The photocurrent of a Si photodiode is measured as a reference for photon density. IPCE was measured for each sample type at visible wavelengths in 10 nm increments for a series of chronoamperometric scans at

various potentials. Figure S5 shows IPCE results measured in Ar-saturated 1M NaOH at 0.4 V *vs Ag/AgCl*.

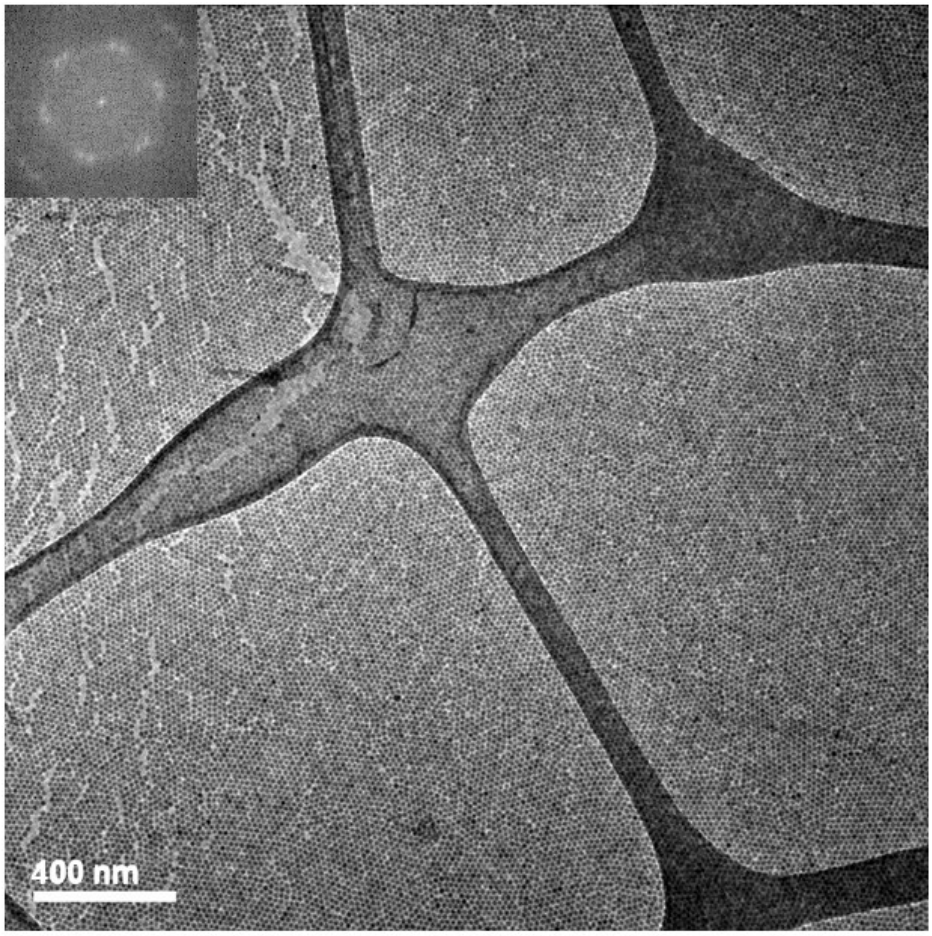

Figure S1 TEM and FFT of Fe_3O_4 NP Superlattices

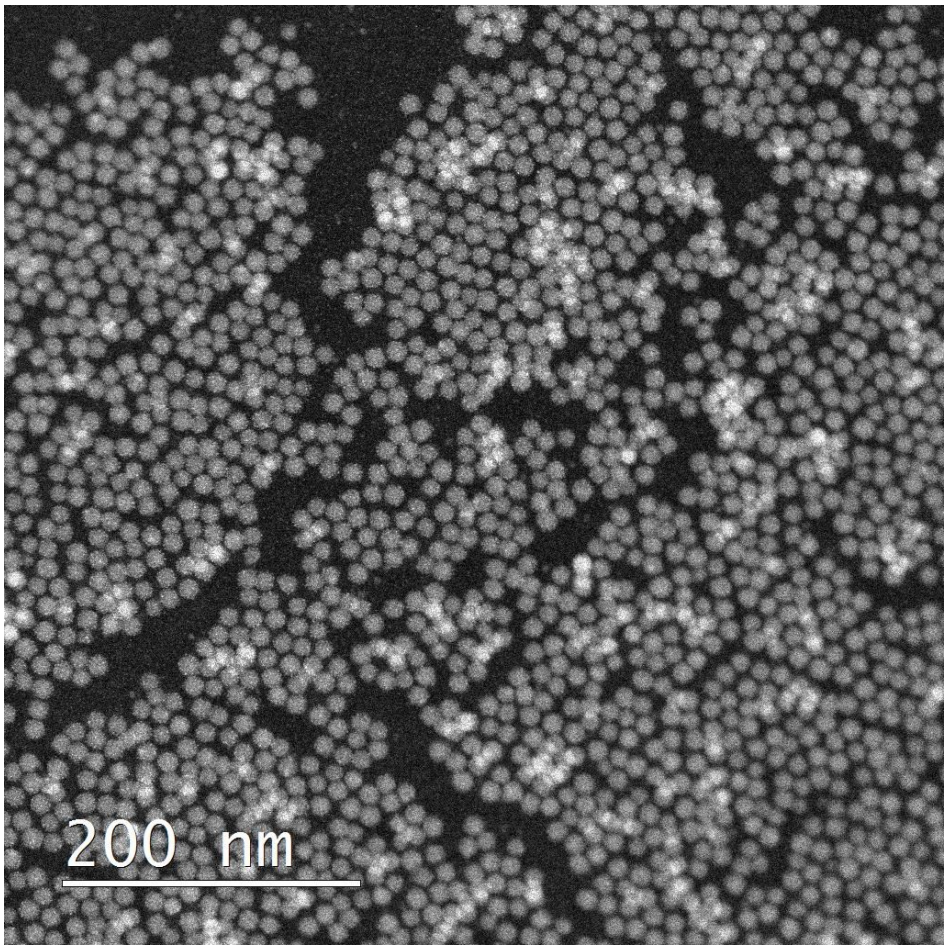

Figure S2 Scanning transmission electron microscopy (STEM) of Fe_3O_4 NP Superlattices formed by drop casting

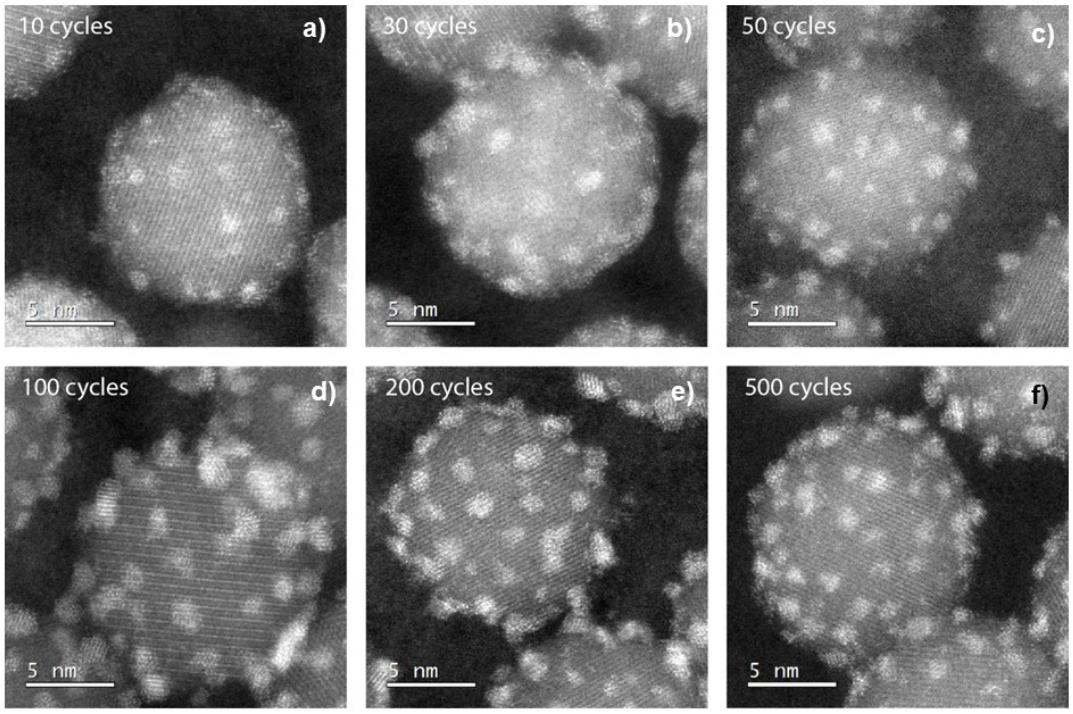

Figure S3 High angle annular dark field (HAADF) high resolution scanning transmission electron microscopy (HR-STEM) images of NPs after 10, 30, 50, 100, 200 and 500 Pt ALD cycles respectively.

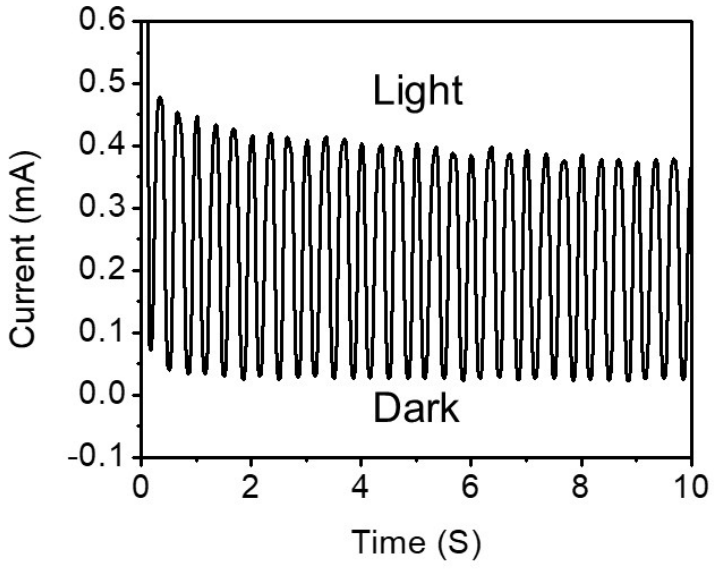

Figure S4 Chronoamperometry with chopped-light illumination (3 Hz). Current was recorded at a constant potential 0.2 V vs. Ag/AgCl with in Ar-satuated 1 M NaOH

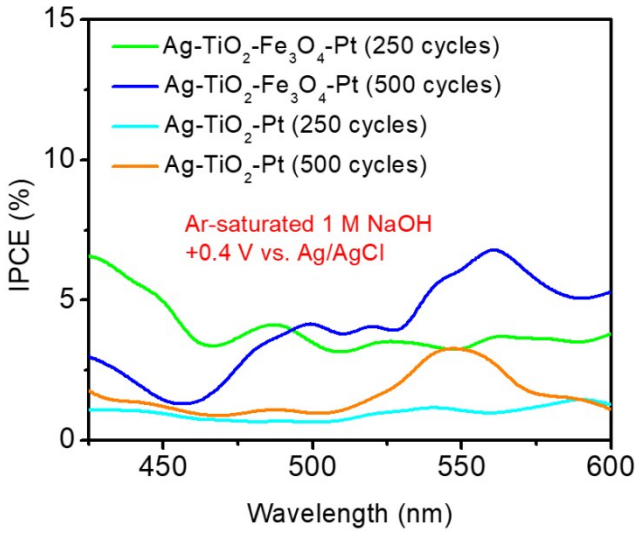

Figure S5 IPCE of Ag-TiO_2-Pt and Ag-TiO_2-Fe_3O_4-Pt with 250 cycles and 500 cycles of ALD

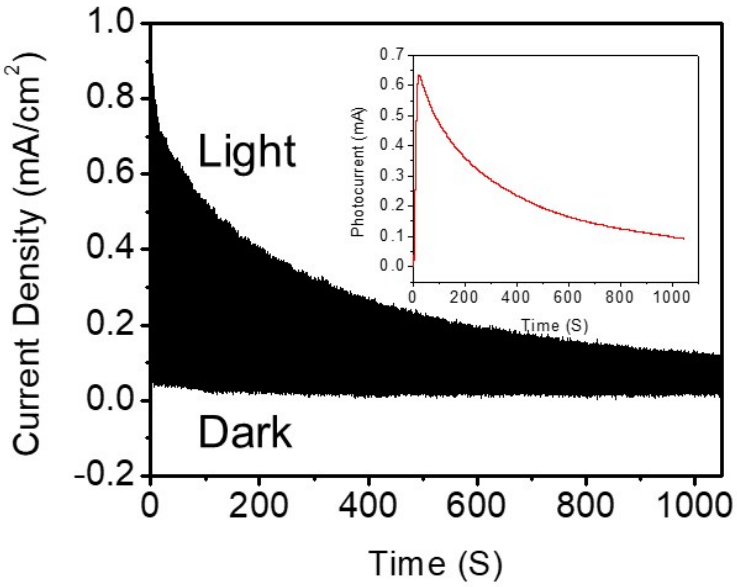

Figure S6 Durability Test of Dark and Light Current Density of Ag-TiO_2-Fe_3O_4-Pt Composites for 1000 Seconds (The inset is the photocurrent)

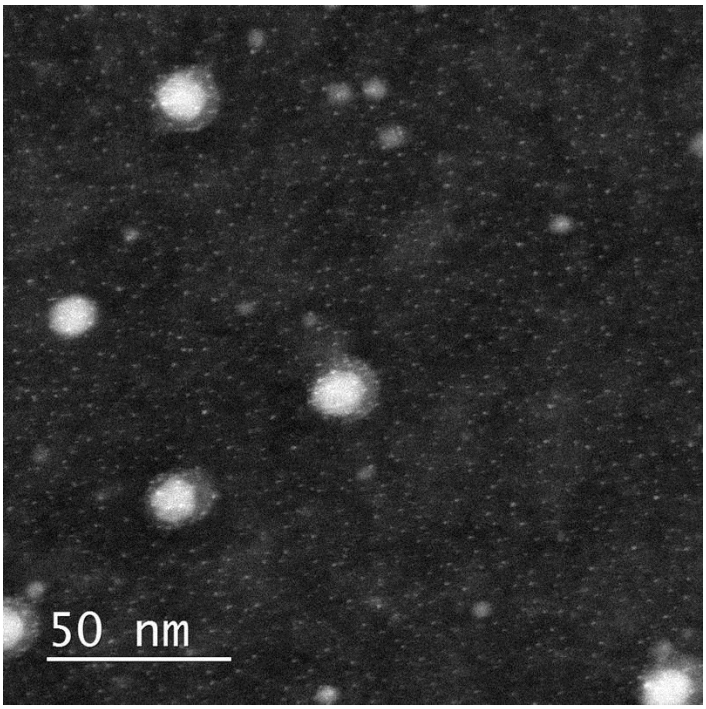

Figure S7 High angle annular dark field (HAADF) high resolution scanning transmission electron microscopy (HR-STEM) images of NPs 500 Pt ALD cycles. In this case the O_2 plasma treatment was insufficient to fully clean the samples. A low contrast (low atomic number) shell can be observed around the Fe_3O_4 particles.

References

[1] J. Park, K. J. An, Y. S. Hwang, J. G. Park, H. J. Noh, J. Y. Kim, J. H. Park, N. M. Hwang, T. Hyeon, *Nature Materials* **2004**, *3*, 891-895.
[2] H. C. M. Knoops, A. J. M. Mackus, M. E. Donders, M. C. M. van de Sanden, P. H. L. Notten, W. M. M. Kessels, *Electrochemical and Solid State Letters* **2009**, *12*, G34-G36.
[3] A. J. M. Mackus, S. A. F. Dielissen, J. J. L. Mulders, W. M. M. Kessels, *Nanoscale* **2012**, *4*, 4477-4480.
[4] A. J. M. Mackus, N. Leick, L. Baker, W. M. M. Kessels, *Chem Mater* **2012**, *24*, 1752-1761.
[5] N. Mulakaluri, R. Pentcheva, M. Scheffler, *J Phys Chem C* **2010**, *114*, 11148-11156.